ISSN 1674-1056
http://cpb.iphy.ac.cn
http://iopscience.iop.org/cpb
中国物理 B
Chinese Physics
中国物理 Chinese Physics B

Hysteresis effect in current-voltage characteristics of Ni/n-type 4H-SiC Schottky structure

Hao Yuan(袁昊), Qing-Wen Song(宋庆文), Chao Han(韩超), Xiao-Yan Tang(汤晓燕), Xiao-Ning He(何晓宁), Yu-Ming Zhang(张玉明), Yi-Men Zhang(张义门)

Citation: Chin. Phys. B . 2019, 28(11): 117303 . **doi:** 10.1088/1674-1056/ab470f
Journal homepage: http://cpb.iphy.ac.cn; http://iopscience.iop.org/cpb

What follows is a list of articles you may be interested in

Influence of deep defects on electrical properties of Ni/4H-SiC Schottky diode

Jin-Lan Li(李金岚), Yun Li(李赟), Ling Wang(汪玲), Yue Xu(徐跃), Feng Yan(闫锋), Ping Han(韩平), Xiao-Li Ji(纪小丽)

Chin. Phys. B . 2019, 28(2): 027303 . **doi:** 10.1088/1674-1056/28/2/027303

Fabrication and characterization of the normally-off N-channel lateral 4H-SiC metal-oxide-semiconductor field-effect transistors

Qing-Wen Song(宋庆文), Xiao-Yan Tang(汤晓燕), Yan-Jing He(何艳静), Guan-Nan Tang(唐冠男),Yue-Hu Wang(王悦湖), Yi-Meng Zhang(张艺蒙), Hui Guo(郭辉), Ren-Xu Jia(贾仁需),Hong-Liang Lv(吕红亮), Yi-Men Zhang(张义门), Yu-Ming Zhang(张玉明)

Chin. Phys. B . 2016, 25(3): 037306 . **doi:** 10.1088/1674-1056/25/3/037306

Low specific contact resistance on epitaxial p-type 4H-SiC with a step-bunching surface

Han Chao, Zhang Yu-Ming, Song Qing-Wen, Tang Xiao-Yan, Zhang Yi-Men, Guo Hui, Wang Yue-Hu

Chin. Phys. B . 2015, 24(11): 117304 . **doi:** 10.1088/1674-1056/24/11/117304

Effect of additional silicon on titanium/4H-SiC contacts properties

Zhang Yong-Ping, Chen Zhi-Zhan, Lu Wu-Yue, Tan Jia-Hui, Cheng Yue, Shi Wang-Zhou

Chin. Phys. B . 2014, 23(5): 057303 . **doi:** 10.1088/1674-1056/23/5/057303

High-performance 4H-SiC junction barrier Schottky diodes with double resistive termination extensions

Zheng Liu, Zhang Feng, Liu Sheng-Bei, Dong Lin, Liu Xing-Fang, Fan Zhong-Chao, Liu Bin, Yan Guo-Guo, Wang Lei, Zhao Wan-Shun, Sun Guo-Sheng, He Zhi, Yang Fu-Hua

Chin. Phys. B . 2013, 22(9): 097302 . **doi:** 10.1088/1674-1056/22/9/097302

Hysteresis effect in current–voltage characteristics of Ni/n-type 4H-SiC Schottky structure*

Hao Yuan(袁昊), Qing-Wen Song(宋庆文)†, Chao Han(韩超), Xiao-Yan Tang(汤晓燕), Xiao-Ning He(何晓宁), Yu-Ming Zhang(张玉明), and Yi-Men Zhang(张义门)

School of Microelectronics, Xidian University, Xi'an 710071, *China*

(Received 12 August 2019; revised manuscript received 16 September 2019; published online 30 October 2019)

Hysteresis current–voltage (I–V) characteristics are often observed in a highly non-ideal ($n > 2$) as-deposited nickel (Ni)/4H-SiC Schottky contact. However, we find that this kind of hysteresis effect also exists in an as-deposited Ni/n-type 4H-SiC Schottky structure even if the ideality factor (n) is less than 1.2. The hysteresis I–V characteristics is studied in detail in this paper by using the various measurements including the hysteresis I–V, sequential I–V sweeping, cycle I–V, constant reverse voltage stress (CRVS). The results show that the hysteresis I–V characteristics are strongly dependent on the sweeping voltage and post-deposition annealing (PDA). The high temperature PDA (800 °C) can completely eliminate this hysteresis. Meanwhile, the magnitude of the hysteresis effect is shown to decrease in the sequential I–V sweeping measurement, which is attributed to the fact that the electrons tunnel from the 4H-SiC to the localized states at the Ni/n-type 4H-SiC interface. It is found that the application of the reverse bias stress has little effect on the emission of those trapped electrons. And a fraction of the trapped electrons will be gradually released with the time under the condition of air and with no bias. The possible physical charging mechanism of the interface traps is discussed on the basis of the experimental findings.

Keywords: 4H-SiC, Schottky, hysteresis I–V, Schottky barrier height

PACS: 73.40.Ns **DOI:** 10.1088/1674-1056/ab470f

1. Introduction

Silicon carbide (SiC) promises to be a candidate for the next-generation high-power devices due to its superior qualities such as the high critical breakdown electric field, high electron saturation velocity, and high thermal conductivity.[1–3] The metal/SiC Schottky contact, as one of the most important basic structures, has aroused great interest for its high switching speed, low forward voltage drop, high performance power devices, which are prompted due to the high demand for the electric power conversion areas such as the power supplies, motor control, electric hybrid vehicles, traction, and electric power transmission.[4,5]

Nowadays, Ti, Ni, Mo, and W contacts are typically employed as the Schottky contacts in the 4H-SiC rectifiers such as the high-voltage JBS diodes.[6–9] The investigation of this contact under the various conditions is essential for a clearer understanding and, eventually, effectively control of these properties. Although the 4H-SiC power Schottky diodes have been commercialized and available for a few years, the current transport and non-ideal I–V characteristics introduced by the spatial inhomogeneity of the barrier height across the Schottky contact area or interface traps, in particular, remain a topic of interest currently.[10–12]

During the last few decades, several investigations concerning the 4H-SiC Schottky contacts have been carried out. For instance, the surface-sensitive 4H-SiC Schottky barrier characteristics and the improvement in ideality factor (n) with silicide formation by different annealing processes are investigated.[13–15] Omar *et al.* reported the experimental observation of the hysteresis in the I–V characteristics of the as-deposited Ni/4H-SiC Schottky diodes.[16] Their results showed that the hysteresis in the I–V curves occurs in a highly nonideal ($n > 2$) as-deposited Ni/4H-SiC Schottky diodes, and they considered that there are a certain number of evenly distributed slow, donor-like interface states existing around the Ni/4H-SiC interface which can induce the hysteresis effect. In contrast, in this paper we find that this kind of the hysteresis effect is also existent in an as-deposited Ni/n-type 4H-SiC Schottky structure even if the value of n is less than 1.2. It is indicated that there are also a number of interface states, which can trap the electrons and exist at the Ni/4H-SiC interface even if the value of n is close to 1 (ideal Schottky contact), which cannot be neglected. Moreover, the possible physical charging mechanism of the interface traps, which can induce the hysteresis I–V characteristics, is not clear either. In our paper, the hysteresis I–V characteristics of the as-deposited Ni/4H-SiC Schottky contact are investigated by the sequential I–V sweeping measurement. The effects of the rapid thermal an-

*Project supported by the National Natural Science Foundation of China (Grant Nos. 61804118, 61774117, and 61774119), the Fundamental Research Funds for the Central Universities, China (Grant Nos. 20101185935 and 20106186647), the National Key Basic Research Program of China (Grant No. 2015CB759600), the Shaanxi Key Research and Development Program, China (Grant No. 2018ZDXM-GY-008), and the Natural Science Basic Research Plan in Shaanxi Province, China (Grant No. 2017JM6003).

†Corresponding author. E-mail: qwsong@xidian.edu.cn

© 2019 Chinese Physical Society and IOP Publishing Ltd

nealing condition on the hysteresis *I*–*V* characteristics are analyzed. Based on previous results and experimental findings by the various electrical measurements, such as the cycle *I*–*V*, constant reverse voltage stress (CRVS) and recovery characteristic, the corresponding physical charging mechanism of the interface trap is discussed in depth.

2. Structure fabrication

In this work, the Schottky structure was fabricated on an N-type, 4° off (0001) oriented 4H-SiC wafer, of which the thickness and doping concentration of the n-type epitaxial layer were approximately 5 μm and 1×10^{16} cm^{-3}, respectively. The thickness and resistivity of the n^+ type 4H-SiC substrate were 380 μm and 0.023 Ω·cm, which was purchased from the Epi World International Co. Ltd. The wafer was first cleaned by the standard Radio Corporation of America (RCA) cleaning, and then dipped into a diluted hydrofluoric acid solution to remove the native oxide from the 4H-SiC surface. Ni was sputtered on the back of the wafer for the cathode. The Ohmic contact was annealed at 1000 °C for 5 min in Ar by using a rapid thermal processing (RTP) system. After forming the back Ohmic contact, an Ni (200 nm in thickness) film was deposited and patterned to form a front Schottky contact. The Schottky contact had a circular geometry with a diameter of 150 μm. Then, the wafer was cut into four samples. A rapid thermal annealing was carried out at 350, 500, and 800 °C, separately, in Ar environment to study the effect of the annealing on hysteresis effect. A set of samples without annealing is denoted as D0, and other three sets of the samples annealed in Ar ambient at 350, 500, and 800 °C, respectively, are denoted as D350, D500, and D800, respectively.

The hysteresis *I*–*V*, sequential *I*–*V* sweeping, cycle *I*–*V*, and CRVS were investigated by using the Agilent B1505 A power device analyzer. And all the *I*–*V* electrical measurements are performed in voltage sweep steps of 100 mV at room temperature.

3. Results and discussion

3.1. Hysteresis *I*–*V* in as-deposited Schottky contact

Figure 1 shows the initial typical hysteresis *I*–*V* characteristic curve of the as-deposited Ni/4H-SiC Schottky contact, which is obtained by forward sweeping the the bias from 0 V to 1.6 V and then backward sweeping. It can be seen that there is an obvious hysteresis voltage. The *n* and Schottky barrier height (SBH) are obtained by fitting the linear part of the forward *I*–*V* characteristics, based on the following equations

$$J = A^* T^2 \mathrm{e}^{-q\phi_\mathrm{B}/kT} \mathrm{e}^{qV/nkT}, \tag{1}$$

$$n = \frac{q}{kT}\frac{\mathrm{d}V}{\mathrm{d}\,(\ln J)}, \tag{2}$$

$$\phi_\mathrm{B} = \frac{kT}{q}\ln\left(\frac{A^* T^2}{J_0}\right), \tag{3}$$

where A^* is the Richardson constant, k is the Boltzmann constant, V is the forward-bias voltage, and T is the absolute temperature.

The values of *n* and SBH from the forward and backward sweeping measurements are both shown in Fig. 1. As can be seen in the figure, sweeping direction (forward or backward) has no significant influence on the value of *n* (1.16), whereas it dramatically enhances the SBH. The SBH extracted from the forward sweeping curve is 1.46 eV, while that extracted from the reverse sweeping curve increases to 1.54 eV. As is well known, the interface traps can modulate the SBH. The increment in SBH might be attributed to the fact that the carriers are trapped at the Schottky interface in the forward voltage sweeping process.

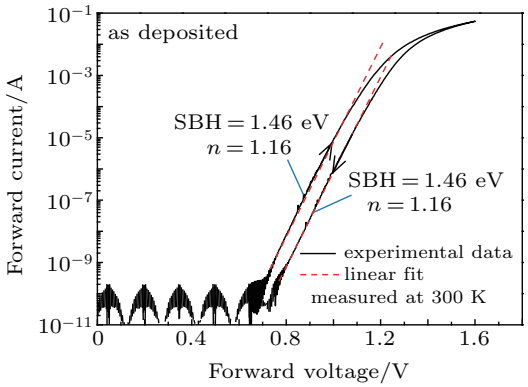


Fig. 1. Typical hysteresis *I*–*V* characteristic curve obtained by forward sweeping bias from 0 V to 1.6 V and then backward sweeping.

To further study the property of the hysteresis effect in the as-deposited Ni/4H-SiC Schottky contact sample, the sequential hysteresis *I*–*V* curves of the D0 sample by being swept three times are obtained. The voltage is swept from 0 V to 2 V first (1st sweeping), then from 2 V to 0 V (2nd sweeping), finally from 0 V to 2 V (3rd sweeping). There is no time staying at 2-V point.

Figure 2 shows the typical three-time sweeping *I*–*V* characteristic curves of the D0 sample, exhibiting a larger hysteresis voltage between the 1st (forward) sweeping and 2nd (backward) sweeping curves. However, in the following 3rd (forward) sweeping, the hysteresis voltage between the 3rd forward sweeping and 2nd backward sweeping curve is very small. It is believed that the larger hysteresis (between 1st and 2nd sweepings) is mainly attributed to the fact that the electrons are trapped by the interface traps at the Ni/4H-SiC interface. After the initial measurement, a number of electrons are trapped in those traps, and most of the trapped electrons cannot be released in the following 2nd backward sweeping, only a fraction of the trapped charges with smaller time constant can be de-trapped during the backward sweeping. Therefore, the initial *I*–*V* curve cannot be obtained again during the later measurements. Although there is no time staying at 2 V in the *I*–*V* sweeping process, sweeping process can be regarded

as a short-time forward-bias stressing process. Therefore, it is concluded that the trapped electrons fill the interface traps at the Ni/4H-SiC interface by the first forward voltage sweeping, and most of the trapped electrons cannot be de-trapped instantly. Moreover, it can be seen that although the value of n is closer to the ideal value, there are also a number of interface states, which can induce the hysteresis I–V characteristics and exist at the Ni/4H-SiC interface for the as-deposited Ni/n-type 4H-SiC Schottky structure.

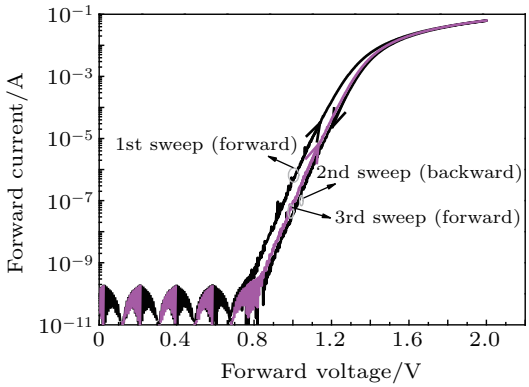


Fig. 2. Typical three-time sweeping I–V characteristic curves of as-deposited sample.

3.2. Effect of rapid thermal annealing on hysteresis

To study the effects of the annealing on the hysteresis I–V characteristics of the Ni Schottky contacts. The as-deposited Ni/4H-SiC Schottky samples are investigated by 5-min rapid thermal annealing (RTA) process at 350 °C, 500 °C, and 800 °C, respectively.

Figure 3 shows the typical hysteresis I–V characteristics obtained under the forward and backward voltage sweeping for the as-deposited, 350 °C-, 500 °C-, and 800 °C-annealed Ni/4H-SiC Schottky samples, indicating that the RTA process has hardly any influence on the slope of the I–V curve. Whereas it significantly affects the hysteresis I–V characteristics. The hysteresis voltage gradually decreases with the RTA temperature increasing. Annealing at 800 °C can completely eliminate the hysteresis effect.

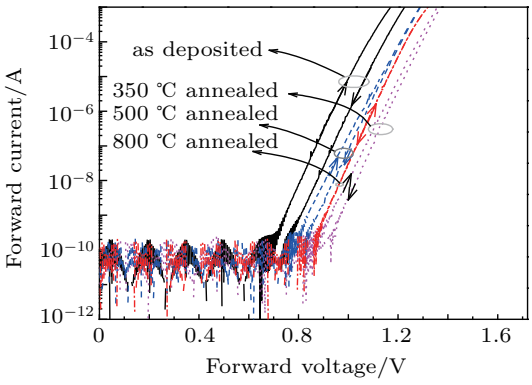


Fig. 3. Typical hysteresis I–V characteristics obtained under forward and backward voltage sweepings for as-deposited, 350 °C-, 500 °C-, and 800 °C-annealed samples.

The typical n and SBH are obtained by fitting the linear part of the forward I–V characteristic curve for each of D0, D350, D500, and D800 samples. Figure 4 shows the rectangular plots of the SBH *versus* the RTA temperature. Each rectangle represents the distribution of the SBH values extracted from the I–V characteristic curves of ten devices. First, it can be seen that the SBH values at the different RTA temperatures are not the same, which might result from the fact that the phases and proportions of the nickel silicide compounds formed under their RTA conditions are different. Moreover, it is obvious that the difference in SBH between the forward and backward sweeping gradually reduces as the RTA temperature increasing. The elimination of the hysteresis effect with high temperature RTA is mainly attributed to the improvement of the interface quality and reduction of those slow interface traps. Figure 5 shows the extracted n as a function of RTA temperature. It is shown that the n can be further improved by the RTA process. The higher RTA temperature makes the n much close to 1. It is generally believed that the improvement of the n with RTA annealing is mainly because of the formation of the stable nickel silicide at the Ni/4H-SiC interface.[17,18] Finally, based on the experimental results and analysis, it can be inferred that the number of the interface traps is mainly dependent on the interface quality, which is determined by the quality of the surface of the epitaxial layer and the deposition process of the metal for the as-deposited metal/n-type 4H-SiC Schottky structure. Therefore, it is indicated that the hysteresis effect is nearly unrelated to the metal species and might appear in the various metals/4H-SiC Schottky contacts widely.

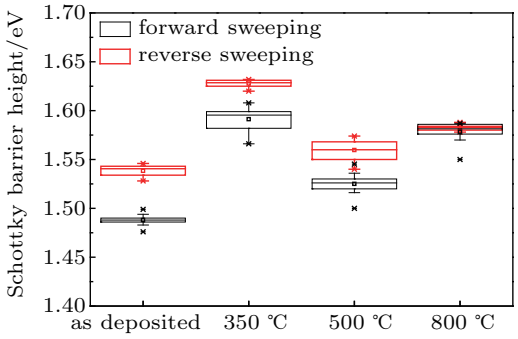


Fig. 4. Rectangular plots of Schottky barrier height *versus* RTA temperature.

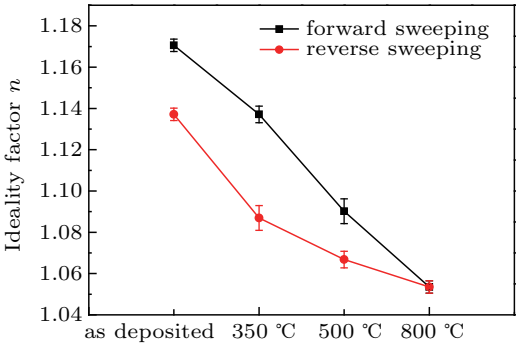


Fig. 5. Plots of extracted ideality factor n *versus* RTA temperature.

3.3. Analysis of charging mechanism

In order to find the charging mechanisms which is responsible for the hysteresis *I–V* characteristic curve, the cycle *I–V*, CRVS and recovery characteristics are investigated.

First, the sequential forward direction *I–V* sweeping measurements are carried out. Figure 6(a) shows the sequential forward direction *I–V* characteristics of the D0 sample. It is shown that the forward *I–V* curves shift toward the high forward voltage and are gradually saturated with scanning time increasing, indicating that the negative charges generate at the interface and the SBH increases. The SBH as a function of the scanning times is presented in Fig. 6(b). It is worthwhile to point that there is a rapid increase of the SBH after the first scanning, implying that the charging process is very short. It is indicated that most of those traps are easily filled under the action of the first forward voltage. Next, it can be seen that the SBH increases slowly and reaches a saturated value with the scanning times increasing.

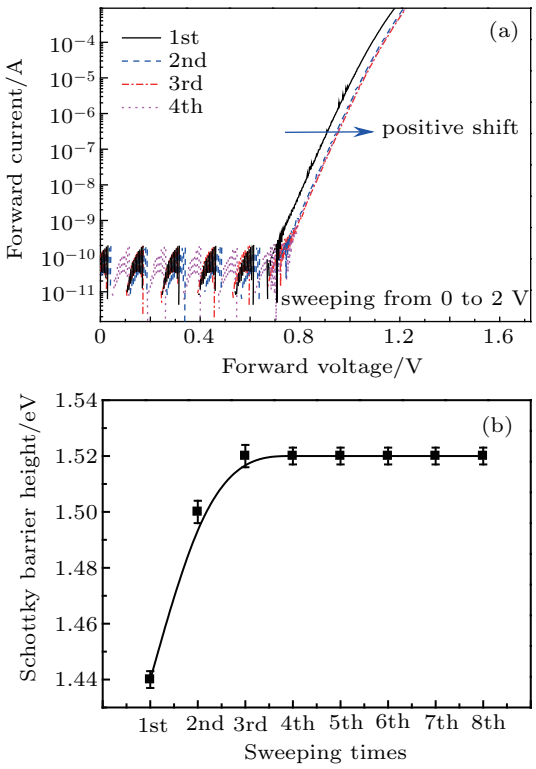


Fig. 6. (a) Sequential forward direction *I–V* characteristics of the D0 sample, and (b) extracted SBH as a function of the scanning times.

To further elucidate the charging mechanism and study the dependence of the charge trapped process on sweeping voltage, the cycle *I–V* measurements are performed at room temperature. Details on this measurement are presented as follows. Voltage is first swept from 0 V to 1 V, and then swept from 0 V to 1.2 V, extended to 1.4 V, and 1.6 V. Figure 7(a) shows the typical cycle *I–V* measurements of the D0 sample after different sweeping voltages. As observed in Fig. 7(a), the sudden increase at the first scanning disappears and the *I–V* curve shifts gradually toward high forward voltage with the maximum sweeping voltage increasing from 1.0 to 1.6. The SBH as a function of the sweeping voltage is presented in Fig. 7(b), it is obvious that the SBH gradually increases with sweeping voltage increasing. It is indicated that the electrons trapped by the Ni/4H-SiC interface traps are strongly dependent on maximum sweeping voltage. It is implied that the main mechanism of the electrons-capturing process is probably due to the electrons directly tunneling, and those interface traps evenly are distributed at the Ni/4H-SiC interface. Figure 7(a) also shows that the *n* keeps nearly constant in the scanning process.

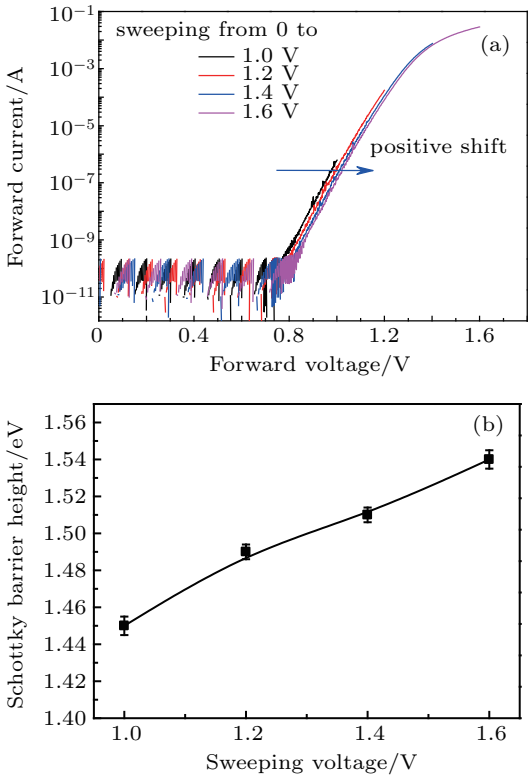


Fig. 7. (a) Typical cycle *I–V* results of D0 sample after different sweeping voltages, and (b) extracted SBH as a function of sweeping voltage.

To study the charge detrapped characteristics and track the recovery regularity of the investigated sructures, the forward *I–V* characteristic curve of the D0 sample, whose SBH and *n* of the fresh state are 1.44 eV and 1.17, respectively, are measured after sequential forward direction *I–V* sweeping measurements (0 V–2 V, 4 times). Figure 8(a) shows the variations of forward *I–V* curve of D0 sample at room temperature after being recovered for 0 day, 3 days, and 7 days, subjected to no bias appilied. The extracted SBH as a function of recovery days is shown in Fig. 8(b). It can be seen that the SBH is gradually recovered toward the initial state after a certain time. At the beginning, the recovery rate of the SBH is relatively fast and then becomes slow, which resembles the variation of SBH

with scanning time as shown in Fig. 6(b). However, it is noteworthy that the SBH is still difficult to achieve the initial value even after 7 days. It may be caused by those trapped charges having a longer time constant, such as "slow" interface traps. In addition, it can be inferred that the releasing mechanism of the part of the trapped electrons may be thermionic emission according to the recovery results.

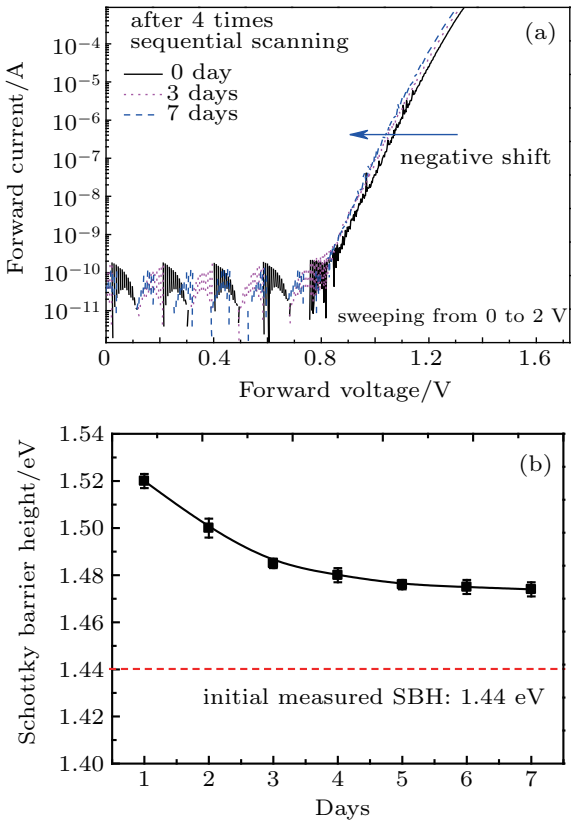


Fig. 8. (a) Typical *I*–*V* curves of D0 sample after sequential forward direction sweeping measurements for three recovery days: 0 day, 3 days, and 7 days, and (b) extracted SBH as a function of recovery days.

Since the positive voltage sweeping can help the electrons fill into the interface traps, the *I*–*V* characteristics of the D0 sample after the negative voltage stress are analyzed too. In this situation, the CRVS measurements are carried out. The stress voltage is fixed at −10 V, and the stress time is set to be 0 s, 60 s, 120 s, 180 s, and 240 s separately. As described before, the D0 sample, whose SBH and n of the fresh state are 1.45 eV and 1.16, respectively, is experimented by the 4-time sequential forward direction *I*–*V* sweeping measurements from 0 V to 2 V before the CRVS measurements. The typical *I*–*V* curves of the D0 sample under the constant voltage stress (−10 V) for different lengths of stressing time and corresponding extracted SBH are presented in Figs. 9(a) and 9(b). It is found that there is almost no difference among the *I*–*V* curves under different lengths of stressing time, indicating that SBH is always unchanged with stressing time increasing for the D0 sample. It is implied that the electrons captured by the interface traps in the Schottky contact region are hardly emitted by the reverse voltage stress, demostrating that the detraping mechanism is not the tunneling.

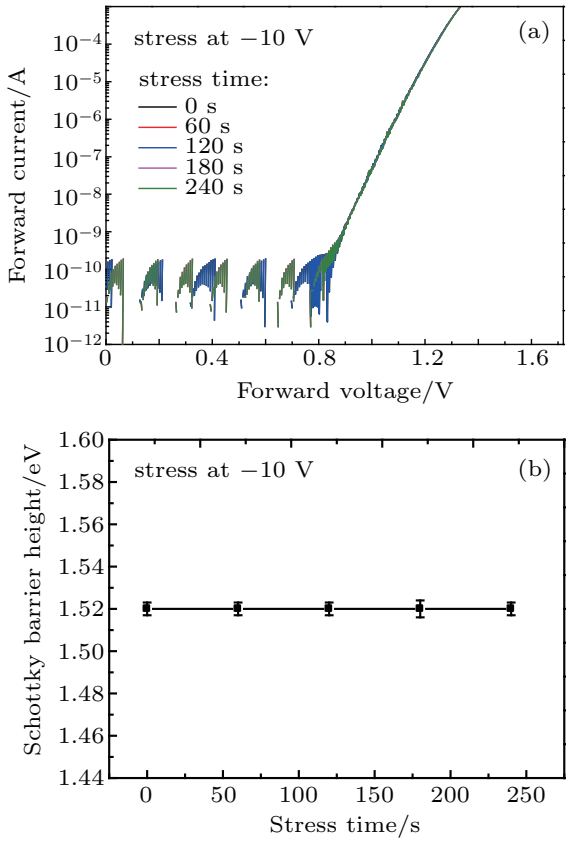


Fig. 9. (a) Typical *I*–*V* curves of the D0 sample under constant voltage stress (−10 V) with different lengths of stressing time, (b) extracted SBH *versus* stressing time.

Based on the above analysis and experimental results, the cause of the hysteresis effect can be identified as the increase of the total negative interface charges. The electrons can be easily trapped by those "slow" interface traps during forward sweeping. However, the trapped electrons are hardly emitted by the reverse voltage stress. The releasing mechanism of the trapped electrons may be the thermionic emission. Schematic representation of the model used to explain the hysteresis effect of Ni/4H-SiC Schottky structure in forward *I*–*V* is shown in Fig. 10. There is one possible mechanism for the electrons to access those slow interface traps. This mechanism involves interface states near the conduction band as the intermediate step. As illustrated in step (I) in Fig. 10, the electrons in 4H-SiC fill those interface states near the conduction band first by tunnelling, and then the trapped electrons leap into the slow interface traps. These acceptor-like traps become negatively charged, thus enhancing the space-charge width on the 4H-SiC side and Schottky barrier height. Meanwhile, those acceptor-like traps have a longer time constant. Once the electrons are captured by these traps, they are hardly emitted during the backward scanning measurement. Therefore, the original curve is no longer obtainable and hysteresis effect appears.

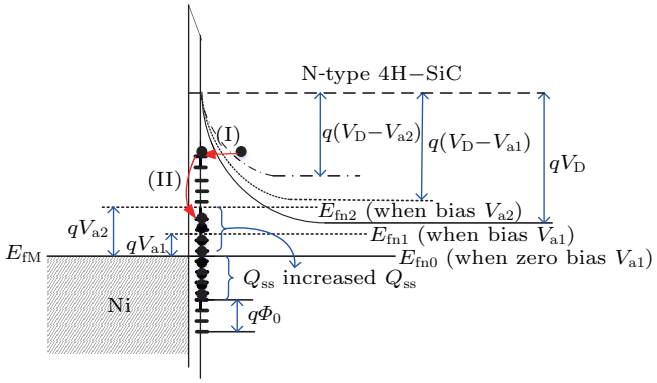


Fig. 10. Schematic representation of the model used to explain hysteresis effect in forward *I–V* of Ni/4H-SiC Schottky contact, showing (I) electrons tunneling from 4H-SiC layer to interface trap, and (II) electrons filling interface states.

4. Conclusions

We systematically investigate the hysteresis *I–V* characteristics of the Ni/4H-SiC Schottky contact. Various measurements including the hysteresis *I–V*, sequential *I–V* sweeping, cycle *I–V*, CRVS, and recovery characteristics are performed to study the properties of the hysteresis effect. First, for the D0 sample, it is found that the SBH can increase from 1.46 eV to 1.54 eV after sweeping the forward bias from 0 V to 1.6 V and then backtoward sweeping in steps of 100 mV, even if the value of n is close to 1. And then there is little hysteresis between 2nd backward sweeping and 3rd forward sweeping, which results from the fact that the trapped electrons fill the interface traps at the Ni/4H-SiC interface by the first forward voltage sweeping. Second, it is shown that the high temperature PDA (800 °C) can completely eliminate this hysteresis effect, of which the SBH keeps unchanged (about 1.58 eV). Finally, based on the cycle *I–V*, CRVS and recovery characteristic measurements, it could be inferred that the main charging mechanism of the interface traps is probably the electrons directly tunneling, and the mechanism of releasing the trapped electrons may be the thermionic emission.

References

[1] Kimoto T 2015 *Jpn. J. Appl. Phys.* **54** 040103
[2] Bhatnagar M and Baliga B J 1993 *IEEE Trans. Electron. Dev.* **40** 645
[3] Alexandrov P, Wright W, Pan M, Weiner M, Jiao L and Zhao J H 2003 *Solid-State Electron.* **47** 263
[4] Zhu L, Chow T P, Jones K A and Agarwal A 2006 *IEEE Trans. Electron. Dev.* **53** 363
[5] Draghici M, Rupp R, Gerlach R and Zippelius B 2015 *Mater. Sci. Forum* **821–823** 608
[6] Wahab Q, Kimoto T, Ellison A, Hallin C, Tuominen M, Yakimova R, Henry A, Bergman J P and Janzén E A 1998 *Appl. Phys. Lett.* **72** 445
[7] Nakamura T, Miyanagi T, Kamata I, Jikimoto T and Tsuchida H 2005 *IEEE Electron Dev. Lett.* **26** 99
[8] Perrone D, Naretto M, Ferrero S, Scaltrito L and Pirri C F 2009 *Mater. Sci. Forum* **615–617** 647
[9] Boussouar L, Ouennoughi Z, Rouag N, Sellai A, Weiss R and Ryssel H 2011 *Microelectron. Eng.* **88** 969
[10] Tumakha S, Ewing D J, Porter L M, Wahab Q, Ma X, Sudharshan T S and Brillson L 2005 *J. Appl. Phys. Lett.* **87** 242106
[11] Calcagno L, Ruggiero A, Roccaforte F and La V F 2005 *J. Appl. Phys.* **98** 023713
[12] Tuokedaerhan K, Tan R, Kakushima K, Ahmet, P, Kataoka Y, Nishiyama A, Sugii N, Wakabayashi H, Tsutsui K, Natori K, Hattori T and Iwai H 2013 *Appl. Phys. Lett.* **103** 111908
[13] Omar S U, Sudarshan T S, Rana T A and Song H 2014 *J. Phys. D: Appl. Phys.* **47** 295102
[14] Pérez R, Mestres N, Montserrat J, Tournier D and Godignon P 2005 *Phys. Status Solidi A* **202** 692
[15] Ewing D J, Wahab Q, Ciechonski R R, Syväjärvi M, Yakimova R and Porter L M 2007 *Semicond. Sci. Technol.* **22** 1287
[16] Omar S U, Sudarshan T S, Rana T A and Song H 2015 *IEEE Electron Dev. Lett.* **62** 615
[17] Kurimoto E, Harima H, Toda T, Sawada M, Iwami M and Nakashima S 2002 *J. Appl. Phys.* **91** 10215
[18] Roccaforte F, La V F, Raineri V, Musumeci P, Calcagno L and Condorelli G G 2003 *Appl. Phys. A* **77** 827